Original Article
http://mjiri.iums.ac.ir
Medical Journal of the Islamic Republic of Iran (MJIRI)

Med J Islam Repub Iran. 2026 (27 Jun);40.68. https://doi.org/10.47176/mjiri.40.68

Potential Renoprotective Effect of Pirfenidone And Silymarin in Acute Kidney Injury Through Targeting miRNA 21

Noha Samir Abdel Latif[1], Tayee, E.M[2], Alsayed A. Abdelhady[3], Manal H. Albadawi[3], Abeer Abdelkader[4], Mostafa Ezz El-Din[2]*, Ahmed Mohammed Taha[2]

Received: 31 Aug 2025 Revised: 26 May 2026 Accepted: 15 Jun 2026 Published: 27 Jun 2026

Abstract

Background: Pirfenidone (PFD) and silymarin (SIL) have demonstrated diverse pharmacological activities and investigated for their renoprotective potential in acute kidney injury (AKI). Their mechanisms involve antioxidant, anti inflammatory, and microRNA mediated pathways. This study evaluated their efficacy against folic acid induced AKI, with emphasis on modulation of miRNA 21.

Methods: 24 adult male albino rats were selected and distributed into four groups . Group 1 (Control): 6 rats received NaHCO3. To induce AKI in the remaining rats, a single dose of folic acid was administered intraperitoneally (250 mg/Kg). Rats were randomly distributed among groups consisting of: Group 2 (50 mg of folic acid was administered intraperitoneally); Group 3 (Administered folic acid and orally treated with pirfenidone at a dosage of 500 mg/kg/day); Group 4 (Administered folic acid and orally treated with silymarin 200 mg/kg/day). Both drugs were administered for three days prior to AKI induction and continued for four days thereafter, the all rats were sacrificed, blood samples were drawn, and renal tissues were harvested for renal function, oxidative stress markers, cytokines (TNF α, TGF β, IL 10), and miRNA 21 expression assessment. Histopathological changes were evaluated by H&E and PAS staining.

Results: Folic acid significantly elevated serum creatinine (2.68±0.10 vs. 0.70±0.06 in controls), urea (83.06±2.97 vs. 30.51±3.55), MDA (3.78±0.19 vs. 1.02±0.07), TNFα (137.36±4.98 vs. 42.15±3.12), and miRNA-21 (2.64±0.13 vs. 1.01±0.05; P<0.050), while reducing SOD (0.64±0.05 vs. 1.92±0.08) and IL-10 (4.39±0.29 vs. 19.87±1.42). Pirfenidone improved renal function (creatinine 1.76±0.04, urea 64.77±1.56), oxidative stress (MDA 2.30±0.04, SOD 1.56±0.09), and cytokines (TNFα 82.28±2.78, IL-10 18.19±1.49). Silymarin produced significantly greater recovery than pirfenidone, with lower creatinine (1.47±0.05 vs. 1.76±0.04; P≤0.050), lower urea (56.89±5.05 vs. 64.77±1.56; P≤0.050), lower MDA (2.07±0.09 vs. 2.30±0.04; P≤0.050), lower TNFα (72.02±3.44 vs. 82.28±2.78; P≤0.050), and reduced miRNA-21 (1.83±0.05 vs. 2.12±0.07; P≤0.050), alongside higher SOD (1.79±0.06 vs. 1.56±0.09; P≤0.050) and IL-10 (21.8±1.54 vs. 18.19±1.49; P≤0.050). Histology confirmed near normal architecture in silymarin treated rats compared to partial recovery with pirfenidone.

Conclusion: Both pirfenidone and silymarin attenuate folic acid-induced acute kidney injury (AKI) through antioxidant, anti inflammatory, and miRNA 21 modulating effects. Silymarin demonstrated more protective effect. These findings support silymarin as a promising candidate for nephroprotection and warrant further mechanistic investigation.

Keywords: Folic acid, AKI, Pirfenidone, Silymarin, MDA, SOD, TNFα, PAS, miRNA 21

Cite this article as: Samir Abdel Latif N, E.M T, Abdelhady AA, Albadawi MH, Abdelkader A, Ezz El-Din M, Mohammed Taha A. Potential Renoprotective Effect of Pirfenidone And Silymarin in Acute Kidney Injury Through Targeting Mirna 21. *Med J Islam Repub Iran.* 2026 (27 Jun);40:68. https://doi.org/10.47176/mjiri.40.68

Corresponding author: Dr Mostafa Ezz El-Din, mustafa.elsayed@med.capu.edu.eg

1. Department of Medical Pharmacology, Faculty of Medicine, Cairo University, El Manial, Cairo 11562, Egypt
2. Department of Medical Pharmacology, Faculty of Medicine, Capital University (formerly Helwan University), Helwan, Cairo 4034572, Egypt
3. Department of Human Anatomy and Evolutionary Biology, Faculty of Medicine, Capital University (formerly Helwan University), Helwan, Cairo 4034572, Egypt
4. Department of Medical Biochemistry and Molecular Biology, Faculty of Medicine, Cairo University, El Manial, Cairo 11562, Egypt

Key Messages:

↑What is "already known" in this topic:

Acute renal failure, also known as acute kidney injury, is frequently seen in critically ill individuals and is linked to elevated risk of mortality with complex and multifaceted pathophysiology. Up till now no specific treatment for controlling such disease.

→What this article adds:

We proved the reno-protective ability of pirfenidone and silymarin in this type of nephropathy, and related for the first time, the effect of microRNA 21 and its relationship with TNF-α and TGF-β in AKI that was improved using each drug generating a testable mechanistic hypothesis that modulation of miRNA-21 is a key node through which antioxidant and antifibrotic therapies limit early profibrotic signaling.

Introduction

Acute kidney injury (AKI) is characterized by a rapid deterioration in the capacity of renal filtration within a brief time. The clinical spectrum of AKI encompasses conditions ranging from modest elevations in serum creatinine (SCr) to severe renal impairment culminating in complete anuric failure (1). AKI remains a profound clinical concern that carries a high risk of adverse outcomes, including elevated morbidity and mortality. Globally, AKI affects in excess of 13 million individuals and is implicated in nearly 1.7 million deaths each year (2, 3). The etiology and pathophysiology of acute kidney injury are intricate and multifaceted, involving hemodynamic alterations, direct tubular toxicity, microvascular obstruction, and renal inflammation. Patients frequently exhibit overlapping pathogenic pathways, posing significant challenges for both accurate diagnosis and effective therapeutic management (4).

As the leading cause of intrarenal AKI, acute tubular necrosis (ATN) is characteristically precipitated by the damage of nephron tubules induced by sepsis, nephrotoxic substances, or drug-induced kidney injury, which is caused by exposure to medications such as non-steroidal anti-inflammatory medications and antibiotics (5, 6). Oxidative stress, ischemia-reperfusion injury, inflammation, and apoptosis are major contributors to disease progression (7). Experimental evidence indicates that administration of high doses of folic acid can precipitate AKI. Excessive folic acid intake perturbs mitochondrial function, compromises antioxidant mechanisms, and enhances the generation of reactive oxygen species (ROS), culminating in renal epithelial cell apoptosis and tubular injury (8).

Short, 22-nucleotide non-coding RNAs known as microRNAs (such as miRNA-21) control the post-transcriptional level of gene expression. They are essential for preserving cellular homeostasis through diverse regulatory functions. Similar to protein-coding genes, the expression of miRNA genes varies depending on tissue type. In certain contexts, miRNAs modulate protein translation to influence apoptosis, proliferation, and differentiation in a cell-type-specific manner (9). MicroRNA-21 plays a distinctive role in wound healing, as it is associated with the phases of inflammation, proliferation, and remodelling. It has been demonstrated to possess anti-inflammatory, anti-apoptotic, and pro-proliferative properties across diverse cell types, while also playing a role in modulating collagen deposition. Increasing evidence suggests that miRNA-21 may influence macrophage polarization through the generation of ROS (10).

Overexpression of microRNA-21 in renal pathology functions as an endogenous activator of Toll-like receptor 7 (TLR7). Activation of this receptor has been associated with kidney disease progression and the pathogenesis of autoimmune and inflammatory disorders. In renal tubular epithelial cells, TLR7 stimulation enhances NF-κB signaling, thereby intensifying pro-inflammatory responses. This mechanism illustrates the link between dysregulated microRNA expression and innate immune activation, highlighting the role of miRNA-21–mediated TLR7 signalling in renal injury and immune dysregulation (11).

Given the current limitations and challenges in the management of AKI, it is essential to investigate the protective efficacy of pharmacological agents capable of mitigating nephrotoxicity. In our study, we assessed the nephroprotective potential of pirfenidone and silymarin. These agents were selected based on their mechanisms of action, which are relevant to renal protection and the regulation of microRNA-21 expression. By targeting different but convergent pathways, pirfenidone and silymarin may offer benefits in attenuating renal injury and modulating key molecular drivers of AKI progression.

Pirfenidone (PFD), a small synthetic pyridone compound, has been approved by the European Medicines Agency and the FDA for idiopathic pulmonary fibrosis treatment (12). While the precise mechanism of action of PFD remains incompletely defined, evidence suggests that it exerts pleiotropic biological effects. Notably, anti-inflammatory and antioxidant impacts, which are thought to support its therapeutic efficacy (13). PFD demonstrates anti-inflammatory activity in the kidney by stabilizing mitochondrial membranes, thereby limiting ROS generation and reducing apoptosis. It further curbs the release of pro-inflammatory mediators, including nitric oxide synthase and cytokines such as interleukin (IL-1β and IL-6) (14, 15). PFD can attenuate the pro-inflammatory and profibrotic responses mediated by microRNA-21-5p through modulation of the transforming growth factor-β (TGF-β)/Smad signalling pathway. By upregulating Smad7 expression, PFD counteracts downstream fibrogenic activity and inhibits fibroblast proliferation in tracheal stenosis (16).

Silymarin (SIL) is an extract of Silybum marianum that contains a diverse array of flavonolignans. It has demonstrated protective effects on neuronal, hepatic, renal, and cardiac tissues, largely attributed to its tissue-regenerating properties. Traditionally, silymarin has been employed as an herbal remedy for liver disorders, and its hepatoprotective activity has been substantiated by numerous experimental studies and supported by several clinical trials (17, 18). Through the downregulation of pro-inflammatory cytokines (IL-4, IL-2, IFN-γ) and mediators such as nitric oxide synthase, together with its protective effects on mitochondrial structure and function by limiting oxidative damage from ROS, SIL exhibits broad antioxidant and anti-inflammatory properties. Moreover, SIL has been shown to downregulate miRNA-21 and induce apoptosis in breast cancer cells, at least in part through suppression of miRNA-21 expression (19, 20).

Methods

Sample size calculation

The sample size of this study was calculated utilizing the G*Power program (Version 3.1.9.2, Franz Faul, Kiel, Germany) (21). The calculation was based on the primary outcome (serum creatinine) using data from prior investigations (Manawy et al., Satyam et al., Zaghlool et al. (22-23). It was assumed that the effect size would be large (Cohen's f = 0.40), with α = 0.05 and power = 0.90. This yielded a

[DOI: 10.47176/mjiri.40.68]

required sample size of 6 rats per group, which was adopted in our design.

Animals and ethical statement

The study utilized twenty-four rats that were procured and maintained in the animal facility of the Faculty of Medicine, Cairo University, Egypt. The animals were housed in plastic cages (33×40×17cm) under standardized environmental conditions, maintained at a temperature of 25±2°C and a relative humidity of 50±5% under a 12:12-hour light-dark cycle with free access to standard chow and drinking water. Every experiment was conducted between 8:00 and 16:00 during the light period. The Institutional Animal Care and Use Committee, Capital University (Formerly Helwan University) (Approval number: 34-2023), in accordance with ARRIVE guidelines and the Guide for the Care and Use of Laboratory Animals protocol (NIH publication) approved the research protocol.

Drugs

(1) Folic acid was provided in the form of powder (MEPACO, Heliopolis, New Cairo, Egypt). Powder was prepared in $NaHCO_3$ and injected intraperitoneally (IP). (2) Pirfenidone was provided in the form of tablets (Cipla, Sikkim, India). The tablets were crushed and dissolved in saline for oral administration. (3) Silymarin was provided in the form of a sachet (SEDICO, 6 October, Egypt) soluble in saline for oral administration.

Experimental design

At the beginning of the study, 24 healthy adult male rats weighing between 200 and 250 grams were used in the baseline of the study. A computer-generated randomization sequence was used to randomly assign animals to groups after a week of acclimatization. To maintain allocation concealment, seven groups (n = 6 each group) were assigned using coded identifiers created by an investigator not involved in outcome assessment as follows:

Group I: Control group (n = 6): Each rat received 2 mL of sodium bicarbonate ($NaHCO_3$) intraperitoneally (IP).

Group II: Acute kidney injury (AKI) group (n = 6): Rats were given a single intraperitoneal injection of 250 mg/kg of folic acid; each rat received 50mg folic acid freshly prepared in 2 mL $NaHCO_3$ on the day of administration (24).

Group III: AKI + Pirfenidone (AKI-PFD) group (n = 6): Before AKI induction, rats received an oral gavage of pirfenidone at a dose of 500 mg/kg/day for three consecutive days, and treatment continued for four days thereafter. Each dose was administered in 1 mL saline (25, 26).

Group IV: AKI + Silymarin (AKI-SIL) group (n = 6): Silymarin was administered to rats at a dose of 200 mg/kg/day by oral gavage for three consecutive days preceding AKI induction, and treatment was sustained for four subsequent days. Each dose was administered in 1 mL saline (27).

On the seventh day of the experiment, all rats were sacrificed. Cervical dislocation was used for scarification under anaesthesia by pentobarbital I.P. injection at a dose of 50 mg/kg body weight (28).

Pretreatment plus short course post-injury dosing was selected to mimic clinically relevant prophylactic and therapeutic strategies, as previously reported in experimental AKI models using pirfenidone and silymarin (29, 30). This regimen reflects translational practices where antioxidant and antifibrotic agents are evaluated both for prevention and early intervention.

The selected doses and treatment duration were determined based on prior pharmacological and toxicological evidence in rodent models, which demonstrated both efficacy and tolerability under similar experimental conditions. Folic acid supplementation has been shown to counteract oxidative stress and telomere attrition in aged rat models (31); Experimental findings indicate that silymarin confers significant hepatoprotective activity, mitigating paracetamol-induced hepatic injury in albino rat models (32). Pirfenidone attenuates acute respiratory distress syndrome fibrosis and inflammation by regulating the transforming growth factor-β activity and production signalling pathways (33).

Measurements

Biochemical tests

Renal function tests

Immediately post-euthanasia, blood was drawn from animals through cardiac puncture in 1.5 ml polypropylene tubes. After centrifuging the blood at 4000× g for 10 minutes, the serum was immediately stored at -20°C to assess the serum level of K and to perform a kidney function test by a colorimetric assay using K, urea, and creatinine detection kits from Bio-Diagnostic Company, Egypt, and assessment was done in accordance with the guidelines provided by the manufacturer.

Preparation of Renal Tissue Homogenates

Using a homogenizer, renal tissue samples were homogenized in ice-cold phosphate-buffered saline (pH 7.4). To isolate the soluble fraction, the homogenates underwent centrifugation, after which the supernatants were meticulously collected and stored until biochemical analysis.

Evaluation of oxidative stress markers (levels of malondialdehyde and superoxide dismutase) in the renal tissue homogenates

The concentrations of oxidative stress markers were assessed using colorimetric assay kits (34, 35). Superoxide dismutase (SOD) activity was measured using the Superoxide Dismutase Detection Kit (Cat. No. SD 25 21, Bio-Diagnostic, Egypt), which is based on the inhibition of nitroblue tetrazolium (NBT) reduction by the superoxide radical. Results were expressed as millimoles per gram of tissue. As an indicator of lipid peroxidation, malondialdehyde (MDA), was quantified by the Malondialdehyde Detection Kit (Cat. No. MD 25 29, Bio-Diagnostic, Egypt), which relies on TBARS, or the thiobarbituric acid reactive substances method. Absorbance was measured at 532 nm, and values were expressed as millimoles per gram of tissue.

[DOI: 10.47176/mjiri.40.68]

Table 1. The sequences of the primers are shown.

Parameter	Primer sequence
MiRNA21 (Accession no. MIMAT0000530)	F: 3'-AGCTTATCAGACTGATGTTG-5'
U6 snRNA (Accession no. M14486.1)	F:3GCTTCGGCAGCACATATACTAAAAT-5'
Universal reverse primer	R: 5'-GTGCAGGGTCCGAGGT-3'

Assessment of cytokines of inflammation (IL10, TNF-α, and TGF-β levels) by ELISA

The levels of inflammatory cytokines interleukin-10 (IL-10), tumor necrosis factor-alpha (TNF-α), and transforming growth factor-beta (TGF-β) were quantified in kidney tissue supernatants using ELISA (enzyme-linked immunosorbent) kits. Specifically, IL-10 was measured with the Cusabio Biotech kit (Cat. No. CSB-E04595r, USA), TNF-α with the Elabscience kit (Cat. No. E-EL-R0019, USA), and TGF-β with the Cusabio Biotech kit (Cat. No. CSB-E04727r, USA). All assays were performed strictly according to the manufacturers' protocols. Standards and samples were added to microplate wells pre-coated with specific antibodies, followed by incubation with biotin-conjugated detection antibodies and horseradish peroxidase (HRP)-streptavidin solution. After washing to remove unbound reagents, substrate solution was added, and color development was monitored. The reaction was terminated with stop solution, and absorbance was measured at 450 nm. Cytokine concentrations were determined from standard curves given in picograms per milliliter (pg/mL) of tissue supernatant.

Assessment of the Expression Level of miRNA21 in the Renal Tissue Homogenates by Quantitative RT-PCR

MiRNA 21 was extracted from renal tissue homogenate using the miRNA extraction kit (Cat. No. # 21300, Norgen Biotek Corp, USA) in accordance with the guidelines provided by the manufacturer. RNA quality was checked using a NanoDrop® 1000 spectrophotometer (NanoDrop Technologies, Inc., Wilmington, USA). Then, for RT-qPCR, the All-in-OneTM miRNA qRT-PCR Detection Kit (Cat. No. QP115, Gene Copoeia, Inc., USA) was used to amplify miRNA21. The PCR reaction protocol was as follows: 94°C for 30s, then 40 cycles of 94°C for 5s and 60°C for 30s. A QRT-PCR system (StepOne, version 2.1, Applied Biosystems, USA) was used to conduct the analysis. The obtained data were used to calculate the expression level of miRNA-21 relative to U6 snRNA as an internal control using the $2^{-\Delta\Delta Ct}$ method (Table 1).

Histopathological Examination of the Kidney

The contralateral kidney was promptly excised, rinsed with cold saline to eliminate residual blood, and fixed in 10% neutral buffered formalin for a minimum of 48 hours at room temperature. Following fixation, specimens were subjected to graded ethanol dehydration (70%, 80%, 95%, and 100%), cleared in xylene, and embedded in paraffin wax. Sections measuring 4–5 µm in thickness were prepared using a rotary microtome and mounted onto glass slides. For general morphology, slides were stained with hematoxylin and eosin (H&E) to assess the seven-domain scale: glomerular injury, tubular epithelial shedding, cytoplasmic vacuolation, nuclear pyknosis, intraluminal casts, interstitial mononuclear infiltration, and vascular congestion. Each domain was evaluated on a scale from 0 to 3 according to the proportion of affected structures per microscopic field (0 = none; 1 = ≤10%; 2 = 11–25%; 3 = >25%). Ten randomly chosen cortical fields from each slide were evaluated under ×200 magnification and verified at ×400 when necessary. Two blinded histologists performed scoring; the mean of both was used for analysis, and inter-rater reliability was assessed by intraclass correlation. Domain scores were summed to obtain a total injury score (max 21). Periodic Acid–Schiff (PAS) staining was performed, highlighting glycogen and glycoprotein components under a light microscope (×200 and ×400 magnifications) (36). Histopathological evaluations were performed under blinded conditions, and biochemical/molecular analyses were likewise conducted on coded samples to ensure blinding of investigators.

Statistical Study

Data were expressed as mean ± standard deviation (SD) for continuous biochemical and cytokine parameters, and as median for semi-quantitative histological scores. The Shapiro–Wilk test was used to assess normality of data distribution.

For normally distributed variables (serum potassium, urea, creatinine, oxidative stress markers, cytokines, and miRNA-21 expression), intergroup comparisons were performed using one-way analysis of variance (ANOVA) followed by Tukey's post hoc test. For histological injury scores, comparisons were performed using the Kruskal–Wallis test followed by Dunn's post hoc test with Bonferroni correction.

Correlation concerning renal miRNA-21 expression and cytokine levels (TGF-β, TNF-α) was determined by Pearson's correlation coefficient (r). Statistical significance was accepted at $P \leq 0.05$ for group comparisons and $P \leq 0.01$ for correlation analyses. All analyses were performed using SPSS 27 and GraphPad Prism 10 (37).

Results

Biochemical results

Impact on Renal Function Tests

Serum potassium, urea, and creatinine levels are summarized in Table 2 and Figure 1. Folic acid–induced AKI (Group 2) produced a significant elevation in serum potassium (5.16±0.18 mmol/L), urea (83.06±2.97 mg/dL), and creatinine (2.68±0.10 mg/dL) compared to the control group (Group 1; $P \leq 0.050$). Both pirfenidone and silymarin significantly reduced serum creatinine, urea, and potassium compared to the AKI group ($P \leq 0.050$). Direct comparison between pirfenidone and silymarin revealed significantly lower creatinine (1.47±0.05 vs. 1.76±0.04; $P \leq 0.05$, Cohen's d=6.42), and urea (56.89±5.05 vs. 64.77±1.56;

[DOI: 10.47176/mjiri.40.68]

Table 2. (Renal function tests) The mean serum K (mmol/L), urea (mg/dl), and creatinine (mg/dl) in various examined groups of male albino rats.

Studied groups	Serum K	Serum urea	Serum creatinine
Group 1 (Control)	3.66 ± 0.09	30.51± 3.55	0.7 ± 0.06
Group 2 (Folic acid- AKI)	5.16 ± 0.18*	83.06 ± 2.97*	2.68 ± 0.1*
Group 3 (AKI- PFD)	4.59 ± 0.05*•	64.77 ± 1.56*•	1.76 ± 0.04*•
Group 4 (AKI- SIL)	4.24 ± 0.03*•	56.89 ± 5.05*•	1.47 ± 0.05*•

Mean ± SD values of serum potassium (mmol/L), urea (mg/dL), and creatinine (mg/dL) in male albino rats across the four studied groups: Group 1 (Control), Group 2 (Folic acid–induced AKI), Group 3 (AKI + Pirfenidone), and Group 4 (AKI + Silymarin). Statistical analyses were conducted using one-way ANOVA followed by appropriate post hoc comparisons. * denotes a significant increase relative to Group 1 (Control), whereas • indicates a significant decrease relative to Group 2 (AKI), with statistical significance set at $P \leq 0.050$.

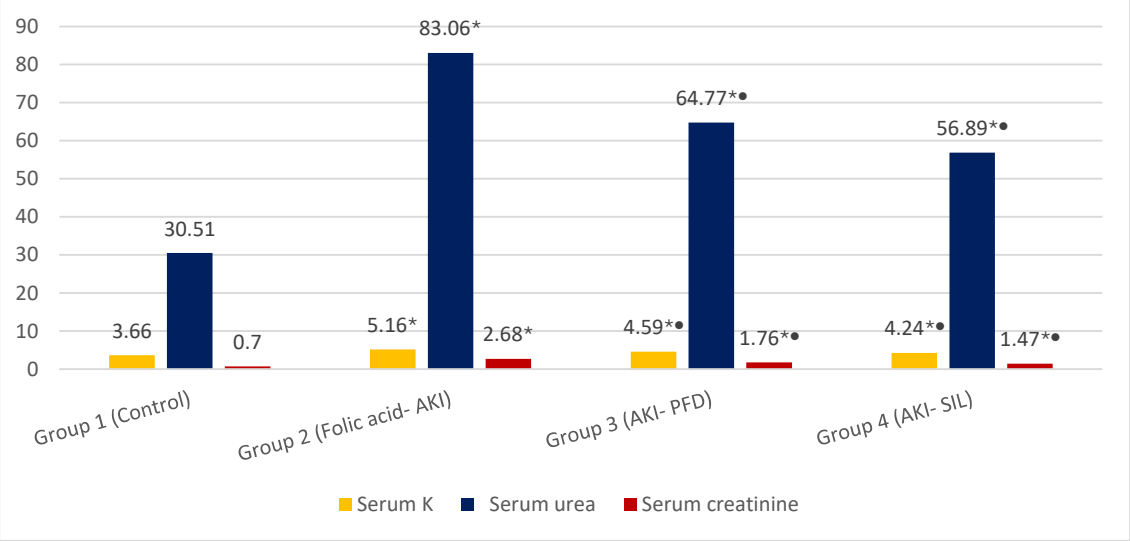

Figure 1. Histogram depicting the mean serum concentrations of potassium, urea, and creatinine across the four experimental groups. Data are expressed as mean ± SD. * indicates a significant increase relative to Group 1 (Control), whereas • denotes a significant decrease relative to Group 2 (AKI), with statistical significance defined at $P \leq 0.050$.

$P \leq 0.050$, Cohen's d=2.11) in the silymarin group with greater improvement than pirfenidone, group.

Impact on Renal Oxidative Stress Markers (SOD & MDA)

Renal malondialdehyde (MDA) and superoxide dismutase (SOD) levels are shown in Figure 2A–B. Group 2 exhibited a significant increase in MDA (3.78±0.19 mmol/g tissue) and a decrease in SOD (0.64±0.05 mmol/g tissue) compared to Group 1 ($P \leq 0.050$). Pirfenidone (Group 3) reduced MDA (2.30±0.04 mmol/g tissue) and increased SOD (1.56±0.09 mmol/g tissue) relative to Group 2 ($P \leq 0.050$). Silymarin (Group 4) produced further improvement, with lower MDA (2.07±0.09 mmol/g tissue) and higher SOD (1.79±0.06 mmol/g tissue) compared to Group 2 ($P \leq 0.050$). Silymarin produced greater improvements vs pirfenidone in oxidative stress markers (MDA 2.07±0.09 vs. 2.30±0.04; $P \leq 0.050$, Cohen's d=3.31); SOD (1.79±0.06 vs. 1.56±0.09; $P \leq 0.050$, Cohen's d=3.01).

Impact on Renal Inflammatory Cytokines (TNF-α, TGF-β & IL 10)

Renal tumor necrosis factor alpha (TNF-α), transforming growth factor beta (TGF-β), and interleukin 10 (IL-10) levels are presented in Figure 3A–C. Group 2 showed significant increases in TNF-α (137.36±4.98 pg/mL) and TGF-β (62.3±2.92 pg/mL), with a decrease in IL-10 (4.39±0.29 pg/mL) compared to Group 1 ($P<0.050$). Pirfenidone (Group 3) reduced TNF-α (82.28±2.78 pg/mL) and TGF-β (54.76±2.27 pg/mL), while increasing IL-10 (18.19±1.49 pg/mL) compared to Group 2 ($P \leq 0.050$). Silymarin (Group 4) produced greater improvement, with lower TNF-α (72.02±3.44 pg/mL) and TGF-β (48.87±2.01 pg/mL), and higher IL-10 (21.8±1.54 pg/mL) compared to Group 2 ($P \leq 0.050$). Silymarin produced greater improvements vs pirfenidone in cytokine balance (TNFα 72.02±3.44 vs. 82.28±2.78; $P \leq 0.050$, Cohen's d=3.28) ;(TGF-β 48.87±2.01 vs. 54.76±2.27; $P \leq 0.050$, Cohen's d=2.88); (IL-10 21.8±1.54 vs. 18.19±1.49; $P \leq 0.050$, Cohen's d=2.38).

Impact on Renal miRNA 21 Expression

Renal miRNA-21 expression levels are shown in Figure 4. Group 2 exhibited a significant increase (2.64±0.13) compared to Group 1 (1.01±0.05; $P<0.050$). Pirfenidone (Group 3) reduced miRNA-21 expression (2.06±0.08; $P \leq 0.050$ vs Group 2), while silymarin (Group 4) produced a further reduction (1.83±0.05; $P \leq 0.050$ vs Group 2). Silymarin produced greater improvements vs pirfenidone in miRNA 21 expression (1.83±0.05 vs. 2.12±0.07; $P \leq 0.050$; Cohen's d=4.77). To explore mechanistic links between cytokines and miRNA-21 expression, within-subject

[DOI: 10.47176/mjiri.40.68]

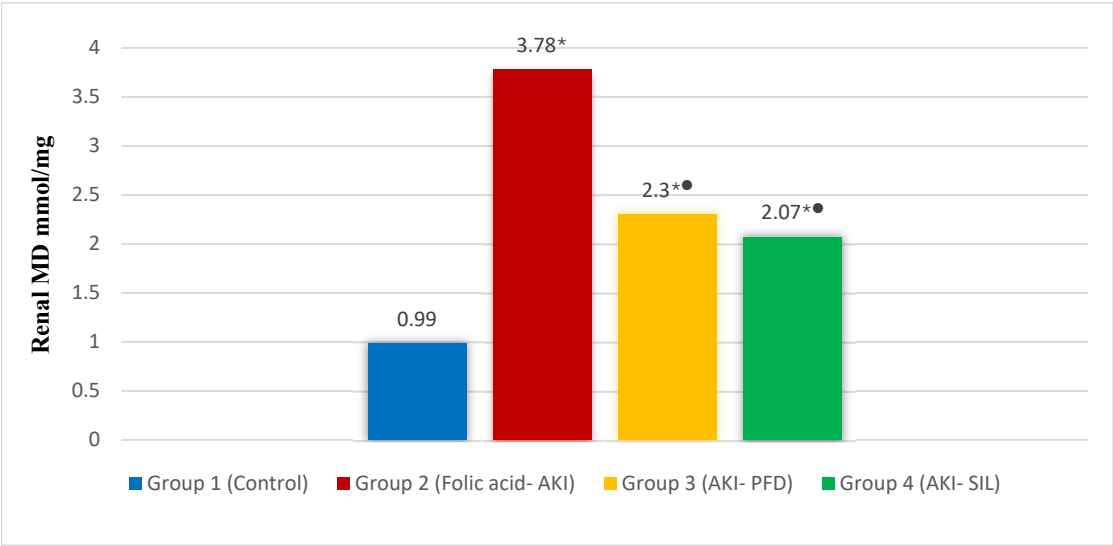

Figure 2A. Histogram showing the mean value of renal MDA concentration (mmol/gm tissue)

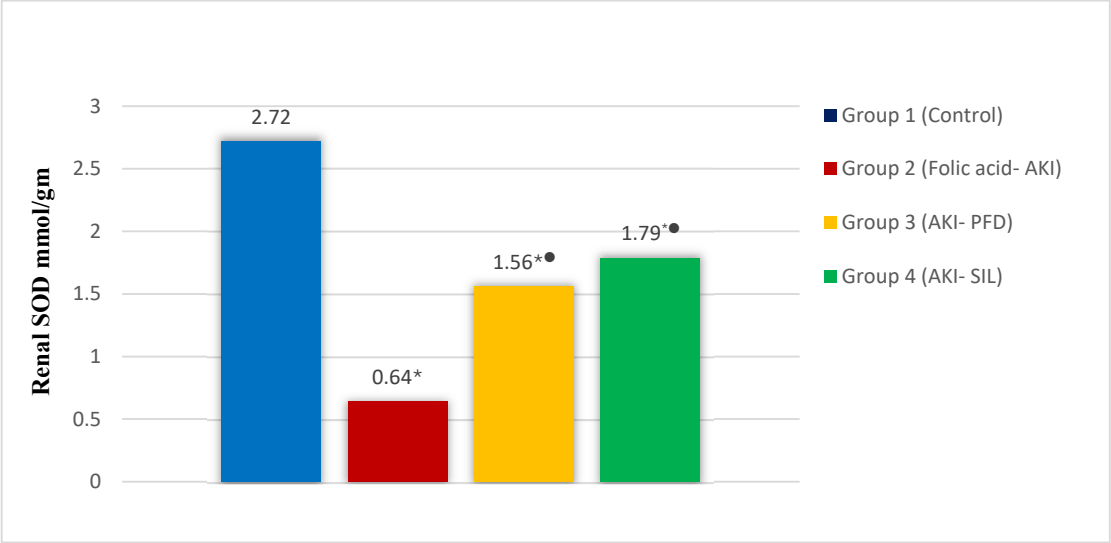

Figure 2B. Histogram showing the mean renal SOD level (mmol/gm tissue)

Figure 2. Markers of renal oxidative stress in the examined groups. (A) Mean malondialdehyde (MDA, mmol/g tissue) levels. (B) Mean superoxide dismutase (SOD, mmol/g tissue) levels. Data are presented as mean ± SD. * indicates significant difference compared to Group 1 (Control); • indicates significant difference compared to Group 2 (AKI) at $P \leq 0.050$.

correlation analyses were performed. Cytokines: miRNA-21 expression correlated positively with TGF-β (r=0.98, $P<0.010$) and TNF-α (r=0.93, $P<0.010$) (Table 3). Scatter plots illustrating these correlations are provided in Figures 5 and 6 with regression lines and 95% confidence intervals shown. These findings demonstrate that higher miRNA-21 expression is consistently associated with increased pro-inflammatory cytokine signalling. This supports the hypothesis that modulation of miRNA-21 is a central node through which pirfenidone and silymarin exert renoprotective effects.

Histopathological results

Assessment of folic acid, pirfenidone, and silymarin effects on Histopathological alterations assessed using hematoxylin and eosin (H&E) staining

Renal histological features are presented in Figure 7. The control group exhibited normal tubular and glomerular architecture (Figure 7a & b); regarding group 2, folic acid triggered distorted renal corpuscles with destruction of glomeruli. Vacuolated cytoplasm, dark-stained pyknotic nuclei, and shedding of some of the tubular epithelial lining cells with separation of tubular cells from the underlying basement membrane. Interstitial mononuclear cellular infiltration is also noticed (Figure 7c). Congested blood vessels (Figure 7d).

[DOI: 10.47176/mjiri.40.68]

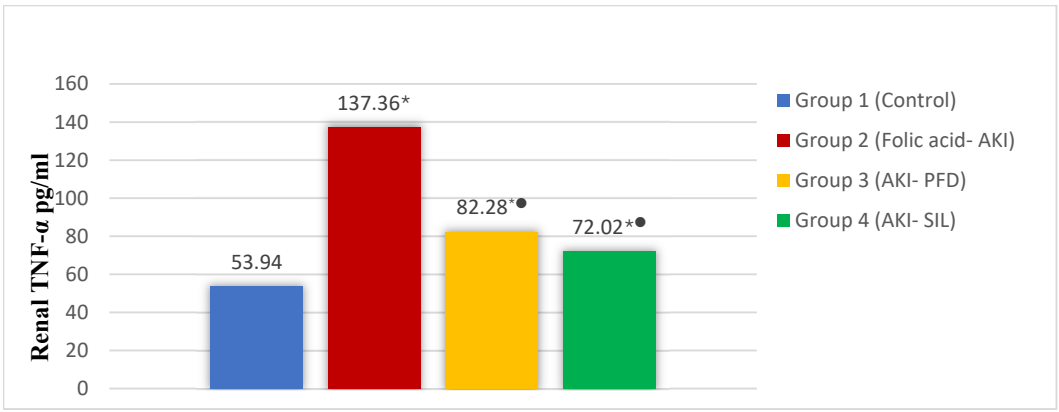

Figure 3A. Histogram showing the mean renal TNF-α (pg/mL tissue) levels

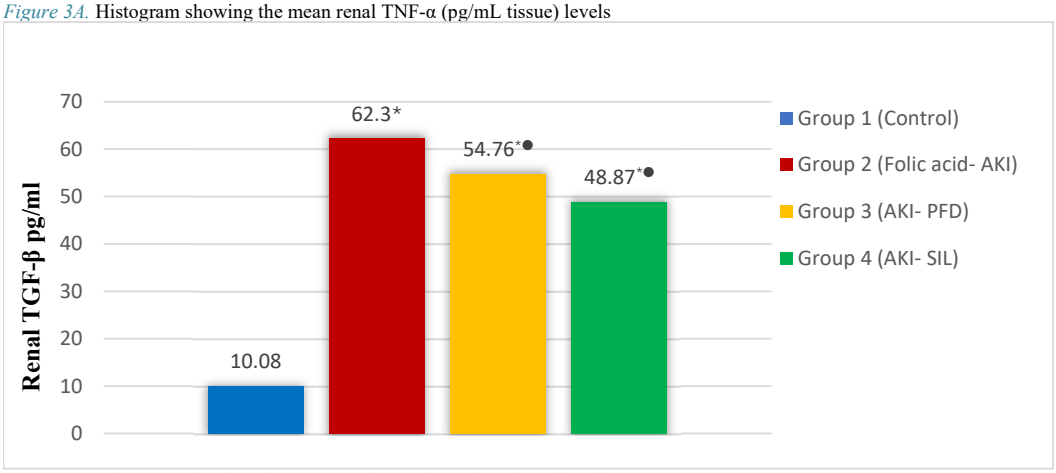

Figure 3B. Histogram showing the mean renal TGF-β (pg/mL tissue) levels

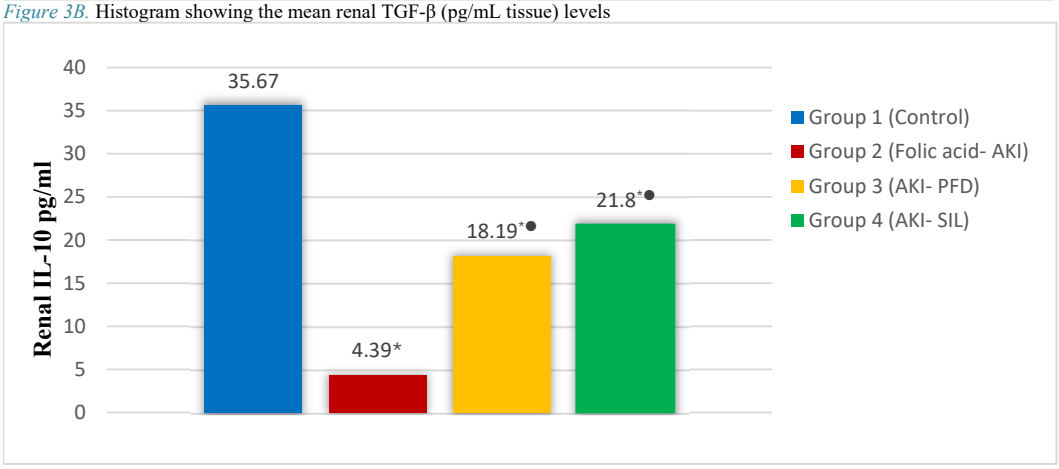

Figure 3C. Histogram showing the mean renal IL-10 (pg/mL tissue) levels

Figure 3. Renal inflammatory cytokine levels in the studied groups. (A) Tumor necrosis factor-α (TNF-α, pg/mL tissue). (B) Transforming growth factor-β (TGF-β, pg/mL tissue). (C) Interleukin-10 (IL-10, pg/mL tissue). Values are mean ± SD. * denotes significant increase compared to Group 1 (Control); • denotes significant decrease compared to Group 2 (AKI) at $P \leq 0.050$.

Pathological changes induced by folic acid were obviously recovered in the AKI pirfenidone-treated group 3, exhibiting few shrunken corpuscles. Many tubular epithelial cells showed vacuoles, and a few tubular cells had dark-stained pyknotic nuclei. Few tubules showed separation of tubular cells from the underlying basement membrane. Congested blood vessels. Few distorted tubules were noticed (Figure 7e). Most tubules showed vesicular nuclei with prominent nucleoli. Homogeneous acidophilic exudate was also noticed (Figure 7f).

Remarkably, pathological changes induced by folic acid noticeably recovered in the AKI Silymarin-treated group 4 to near normal, showing many renal corpuscles were apparently normal; a few appeared shrunken with wide capsular space. Tubules appeared uniform with vesicular nuclei and prominent nucleoli (Figure 7g). Some tubular epithelial

[DOI: 10.47176/mjiri.40.68]

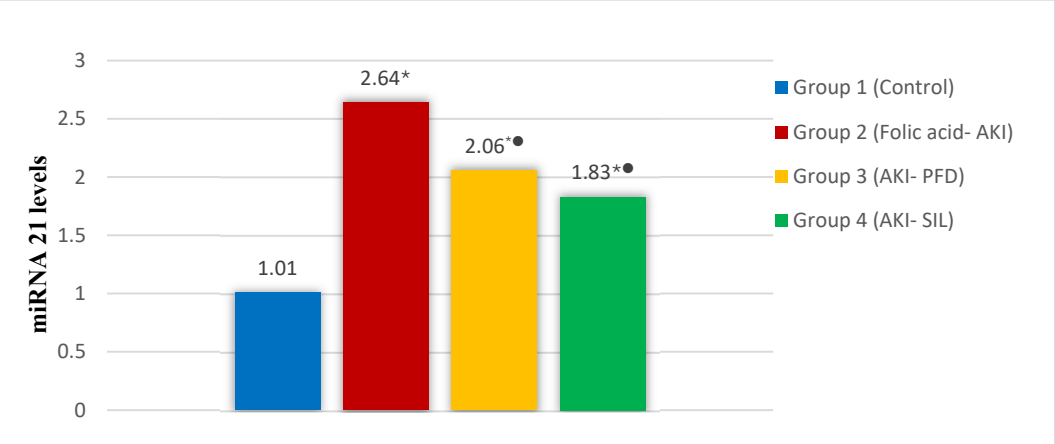

Figure 4. Histogram showing renal expression of miRNA-21
Renal expression levels of microRNA-21 in the four studied groups. The values are presented as mean ± SD. * indicates significant increase compared to Group 1 (Control); • indicates significant decrease compared to Group 2 (AKI) at $P \leq 0.050$.

Table 3. MiRNA 21 expression level in correlation with TGF-β and TNF-α level in group 2 (AKI group).

The correlation between MiRNA 21, TGF-β and TNF- α level in group 2 (AKI)		
Variables	MiRNA 21	
	r	*P*
TGF-β	.982	<0.001
TNF-α	.933	.007

Correlation analysis between renal miRNA-21 expression and cytokine levels (TGF-β, TNF-α) in Group 2 (Folic acid–induced AKI). Pearson correlation coefficients (r) and p-values are shown. Correlation is significant at $P=0.010$.

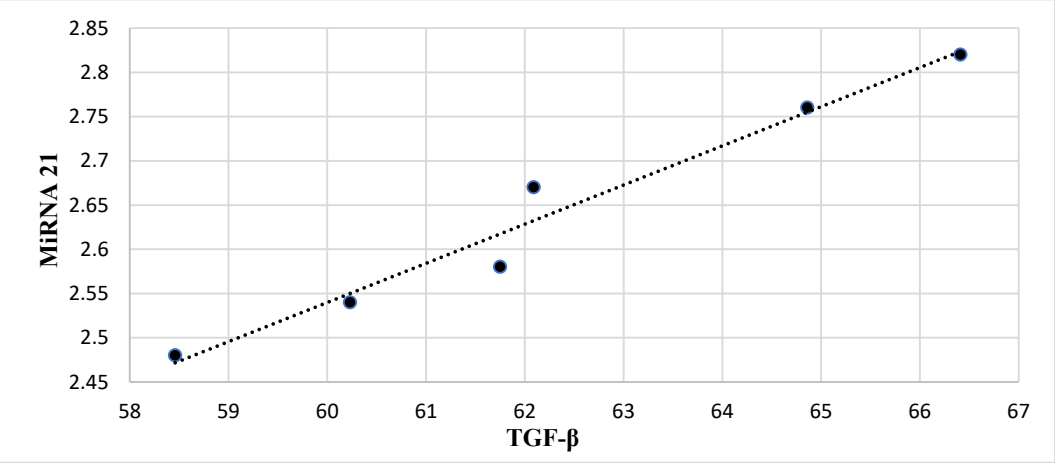

Figure 5. Showing the relation between miRNA 21 and TGF-β
Scatter plot showing the correlation between renal miRNA-21 expression and TGF-β levels. Each point represents one subject. Regression line and 95% confidence interval are shown; analysis revealed a positive correlation (r=0.98, $P=0.010$). Pearson correlation analysis at $P=0.010$.

cells showed vacuolated cytoplasm; few tubular cells had dark-stained pyknotic nuclei. Homogeneous acidophilic exudate with most tubular cells having vesicular nuclei with prominent nucleoli was also noticed (Figure 7h).

Assessment of folic acid, pirfenidone, and silymarin effects on histopathological changes by PAS

Renal histological features are displayed in Figure 8.

The apical brush boundaries of the cells lining the PCTs and DCTs were clearly seen in the control group. Both the tubular basement membrane and the parietal layer of Bowman's capsule demonstrated structural integrity (Figure 8a); regarding group 2, folic acid caused focal areas of lost brush border in some tubular cells with complete loss of the brush border in others. Loss of the tubular basement membrane was evident, manifesting as both focal and complete disruption, accompanied by thickening in certain tubules. In addition, focal thickening was observed in the parietal layer of Bowman's capsule (Figure 8b).

In group 3, the administration of pirfenidone produced improvement in renal histology in the form of many of the renal tubules with intact apical brush borders and basement membranes (Figure 8c). Regarding group 4, treatment with silymarin caused more improvement in renal histology in

[DOI: 10.47176/mjiri.40.68]

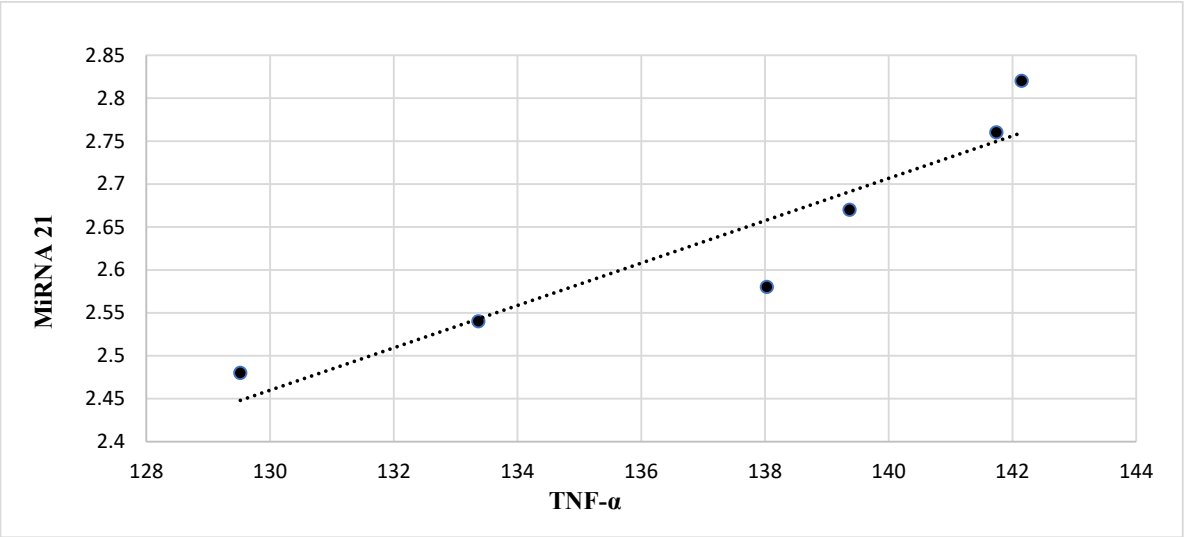

Figure 6. Showing the relation between miRNA 21 and TNF-α
Scatter plot showing the correlation between renal miRNA 21 expression and TNF-α levels across individual rats. Each point represents one subject. Regression line and 95% confidence interval are shown. Pearson correlation analysis revealed a positive correlation (r = 0.93, p = 0.010), with statistical significance defined at *P*=0.010.

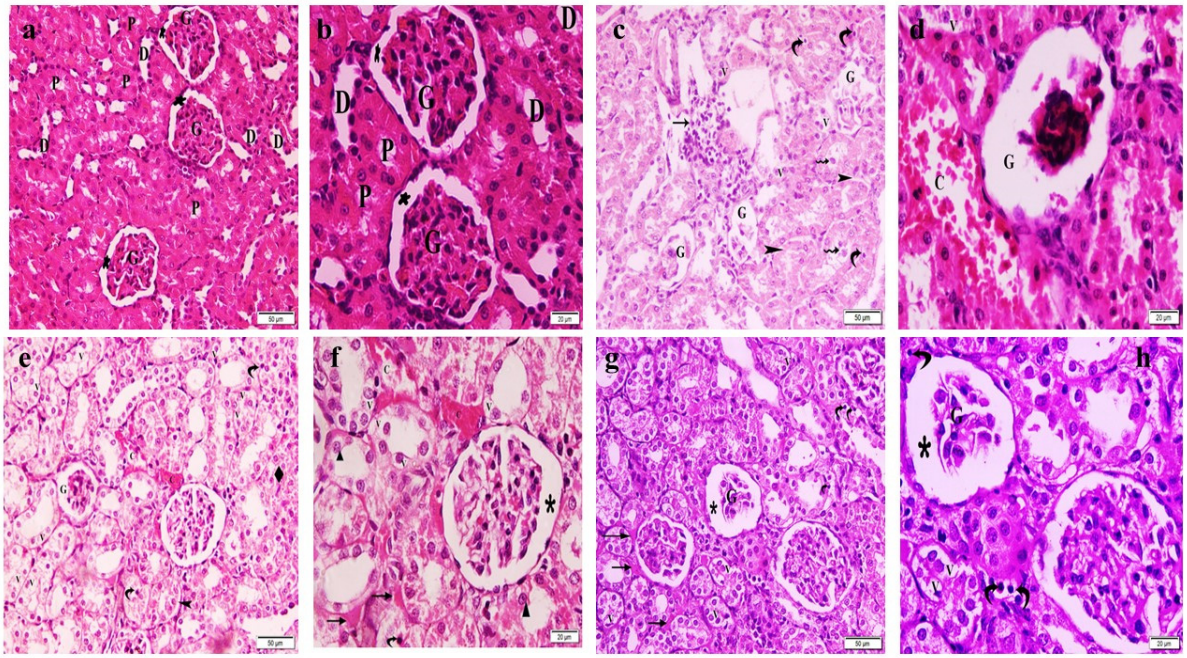

Figure 7. Illustrative hematoxylin and eosin (H&E) stained sections of renal cortex with corresponding semi-quantitative injury scores. (a, b) Control group (score 0) showing normal glomeruli (G), proximal (P) and distal (D) tubules with intact architecture. (c, d) Group 2 (Folic acid–induced AKI; median injury score ~18) showing distorted corpuscles, glomerular destruction, vacuolated cytoplasm (V), pyknotic nuclei (curved arrows), epithelial shedding (spiral arrows), basement membrane separation (arrowhead), mononuclear infiltration (arrow), and congested vessels (C). (e, f) Group 3 (AKI + Pirfenidone; median injury score ~10) showing partial recovery with shrunken corpuscles, vacuolated cytoplasm, occasional pyknotic nuclei, congested vessels, and homogeneous acidophilic exudate. (g, h) Group 4 (AKI + Silymarin; median injury score ~6) showing near-normal architecture with mostly intact corpuscles, uniform tubules, vesicular nuclei, and minimal residual injury. Magnifications: ×200 and ×400.

the form of most of the renal tubules with preserved apical brush borders and basement membranes (Figure 8d, Table 4).

Discussion

In the folic-acid model of AKI, a single high dose of FA produced marked renal dysfunction, oxidative stress, pro-inflammatory cytokine elevation, histological tubular injury, and upregulation of miRNA-21. In this study, pre-treatment with pirfenidone and silymarin significantly

[DOI: 10.47176/mjiri.40.68]

Table 4. H&E histological scoring in all experimental groups.

Group	Glomerular injury	Nuclear pyknosis	Tubular shedding	Vacuolation	exudate	Infiltration	Congestion	Total score
Control (G1)	0	0	0	0	0	0	0	0
Folic acid–AKI (G2)	3 (3–3)	3 (2–3)	3 (2–3)	3 (2–3)	2 (1–2)	3 (2–3)	3 (2–3)	18 (16–20)
AKI + Pirfenidone (G3)	2 (1–2)	1 (1–2)	2 (1–2)	2 (1–2)	1 (0–2)	1 (1–2)	1 (1–2)	10 (8–12)
AKI + Silymarin (G4)	1 (0–1)	1 (0–1)	1 (0–1)	1 (0–1)	1 (0–1)	0 (0–1)	0 (0–1)	6 (5–7)

Values are presented as median based on 10 cortical fields per animal. Each domain was scored on a 0–3 scale (0: none; 1: ≤10%; 2: 11–25%; 3: >25%). Total injury score is the sum of all domains (maximum 21). Statistical analysis was performed; $p \leq 0.050$ was considered significant.

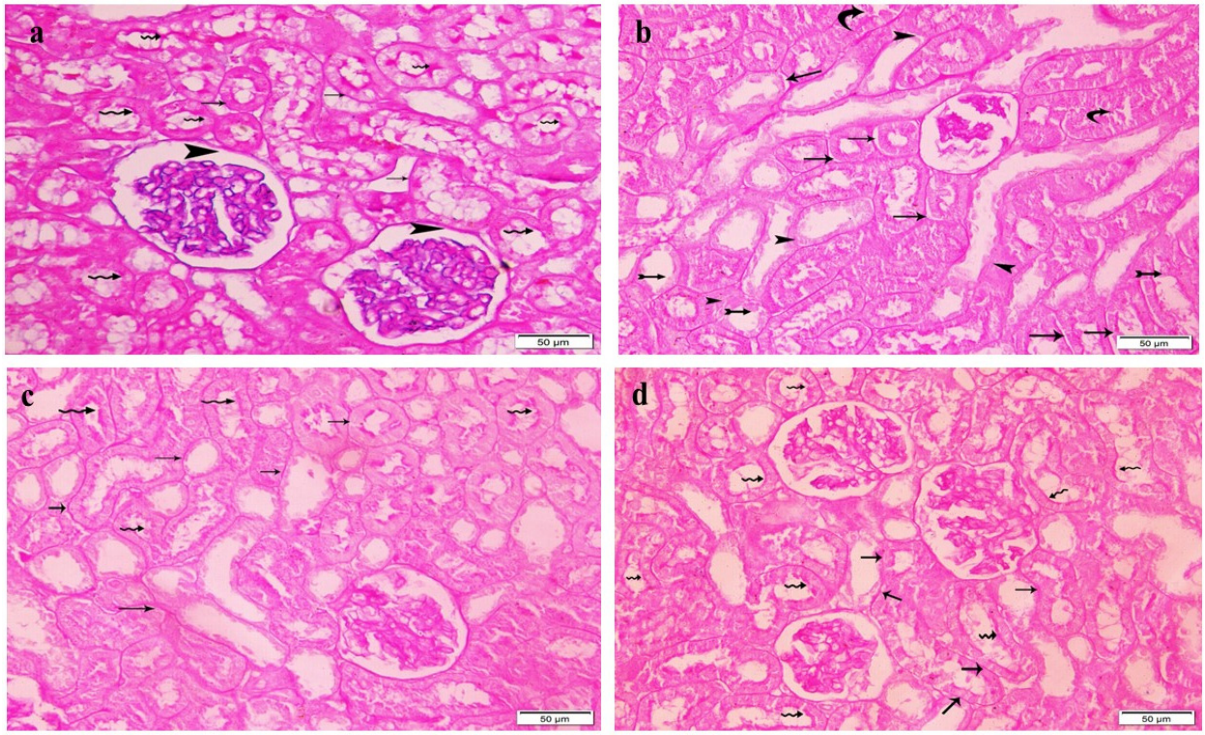

Figure 8. Representative periodic acid–Schiff (PAS) stained sections of renal cortex with brush border and basement membrane scores. (a) Control group showing intact apical brush borders (wavy arrows), preserved basement membranes (arrows), and normal Bowman's capsule (arrowhead). (b) Group 2 (Folic acid–induced AKI) showing focal and complete loss of brush borders (bifid and curved arrows), basement membrane loss/separation (arrowheads), and thickening of Bowman's capsule. (c) Group 3 (AKI + Pirfenidone) showing partial recovery with many tubules retaining brush borders and basement membranes. (d) Group 4 (AKI + Silymarin) showing marked recovery with most tubules preserving brush borders and basement membranes. Magnification ×200.

improved renal function (serum K, urea, creatinine), reduced lipid peroxidation (MDA), restored antioxidant capacity (SOD) and IL10, lowered pro-inflammatory and pro-fibrotic cytokines (TNF-α, TGF-β), improved histological scores, and decreased renal miRNA-21 expression.

Rapid loss of renal function is a hallmark of acute kidney injury (AKI), which is associated with high morbidity and mortality rates. Furthermore, AKI is a recognized risk factor for the development of chronic kidney disease (CKD), underscoring the importance of timely AKI management in mitigating progression toward CKD (38).

In the current study, serum K, urea, and creatinine were utilized as markers of renal function; these parameters were significantly elevated following folic acid administration, likely due to tubular epithelial cell necrosis and the subsequent release of pro-inflammatory cytokines, both of which impair glomerular filtration. These effects were effectively ameliorated by pretreatment with silymarin and pirfenidone. Renoprotective effect of both silymarin and pirfenidone appear to be mediated through antifibrotic, anti-inflammatory, and antioxidant properties (39, 40).

Oxidative stress, defined by excessive accumulation of reactive oxygen species (ROS) and lipid peroxidation as evidenced by elevated malondialdehyde (MDA) levels and concomitant depletion of superoxide dismutase (SOD), acts as a principal mediator of tissue injury in the folic acid-induced model. In our study, both pirfenidone and silymarin reversed these biochemical signatures, a result consistent with their established antioxidant mechanisms. Pirfenidone likely stabilizes mitochondrial membranes and reduces ROS generation, whereas silymarin exerts dual antioxidant actions, functioning as a direct free-radical scavenger while simultaneously enhancing endogenous antioxidant defense mechanisms. These findings are concordant with prior investigations that have demonstrated the protective efficacy of both pirfenidone and silymarin in attenuating oxidative

[DOI: 10.47176/mjiri.40.68]

stress-mediated injury across a range of experimental models (41, 42).

Furthermore, the FA model provoked a pro-inflammatory and pro-fibrotic milieu, characterized by elevated TNF-α and TGF-β alongside reduced IL-10. Both treatments shifted this balance toward resolution; the observed reductions in TNF-α and TGF-β, coupled with increased IL-10, are consistent with attenuated pro-fibrotic signalling and enhanced anti-inflammatory regulation. These cytokine shifts provide a plausible mechanistic link between biochemical recovery (improved renal function and reduced MDA) and histological preservation (mitigated tubular necrosis and preserved brush borders), supporting the interpretation that these agents effectively mitigate both acute injury and early pro-fibrotic responses.

This aligns with previous studies suggesting the efficacy of pirfenidone in inhibiting inflammatory responses and its capacity to increase the production and emission of IL-10. Furthermore, its anti-fibrotic effects have been shown to significantly decrease collagen deposition (43-45).

Moreover, the anti-inflammatory and anti-fibrotic actions of Silymarin ere referred to as being through inhibition of NF-κB, 5-lipoxygenase, and COX, alongside the upregulation of IL-10 expression. Silymarin also modulates the TGF-β/SMAD signalling pathway to effectively inhibit TGF-β1 expression, thereby suppressing fibrotic progression (46, 47).

Renal miRNA-21 expression was significantly upregulated following FA-induced injury and was effectively reversed by both pirfenidone and silymarin treatments. Rather than functioning as a unidirectional biomarker, miRNA-21 is increasingly recognized for context-dependent roles in renal pathophysiology. While transient upregulation may facilitate initial cellular repair, its sustained overexpression in the FA model is considered a hallmark of maladaptive repair. This maladaptive response drives the progression toward chronic injury by amplifying pro-fibrotic signalling through the TGF-β/Smad pathway. Consequently, the observed suppression of miRNA-21 by pirfenidone and silymarin suggests that these agents exert their renoprotective effects, in part, by intercepting the signalling cascade responsible for the progression from acute injury to chronic fibrosis.

In the present model, the strong positive correlations observed between renal miRNA-21 expression and pro-fibrotic and pro-inflammatory cytokines (TGF-β and TNF-α) support a predominantly maladaptive role for miRNA-21 in FA-induced injury. Although our correlation revealed significant associations between miRNA-21 expression, oxidative stress and cytokine levels, these findings should be interpreted with caution. Correlation does not establish causation, and the observed relationships may reflect indirect or multifactorial pathways. Recent studies emphasize that miRNA-21 plays complex regulatory roles in kidney injury, but causal inference requires targeted experimental validation (48). Future work employing genetic modulation of miRNA-21 will be necessary to confirm causal links.

The observed reduction of renal miRNA-21 expression by pirfenidone and silymarin aligns with their established anti-fibrotic and anti-inflammatory properties, suggesting that the regulation of this microRNA expression may represent a key mechanism through which these agents limit the progression toward chronic fibrosis. This interpretation reconciles apparent contradictions in the literature by emphasizing the importance of timing and physiological context; while early, transient miRNA-21 induction may facilitate reparative processes, sustained elevation driven by ongoing oxidative stress and pro-inflammatory signalling promotes fibrotic progression and adverse renal outcomes.

The capability of both agents to suppress miRNA-21 expression aligns with previous studies demonstrating that pirfenidone-mediated inhibition of miRNA-21 reduces fibroblast proliferation and pro-inflammatory cytokine release, thereby exerting potent anti-fibrotic effects (49).

The downregulation of miRNA-21 by silymarin has also been demonstrated in a psoriasis model, where it was shown to target the TGF-β/miR-21-5p signalling pathway (50).

According to H&E staining, FA-induced renal affection was characterized by glomerular destruction, vacuolated cytoplasm, epithelial shedding, and mononuclear infiltration. These manifestations of histological injury driven by oxidative stress, cytokine imbalance, and miRNA-21 upregulation are consistent with previous findings (51).

Pirfenidone treatment partially reversed these pathological changes, with the tissue exhibiting fewer shrunken corpuscles and reduced epithelial injury. In contrast, silymarin restored renal architecture to a near-normal state, characterized by intact corpuscles and uniform tubules. This histological recovery supports the hypothesis that both agents exert their effects through antioxidant and anti-inflammatory pathways (52, 53).

PAS staining corroborated these findings; FA administration led to the loss of brush borders and compromised basement membrane integrity. In contrast, pirfenidone preserved many brush borders, while silymarin achieved almost complete restoration. These histological improvements parallel the biochemical recovery, indicating the stabilization of tubular epithelial integrity mediated by decreased ROS and cytokine signalling. Our observations align with Manawy et al. (2024), who demonstrated that pirfenidone improves doxorubicin-induced renal damage through its potent antifibrotic activity (21). The notable histological recovery observed with silymarin aligns with its broader antioxidant profile and more pronounced suppression of miRNA-21. These results are consistent with Deng et al. (2024), who verified the efficacy of silibinin in ameliorating PAS-positive histological changes in an ischemia-reperfusion kidney injury model. This protection was achieved through the suppression of both pro-inflammatory cytokines (IL-1β and TNF-α) and ferroptosis (54).

Our limitations include: the relatively small group size, a singular endpoint measurement (Day 7), which restricts the ability to draw conclusions about the progress of long-term acute kidney injury (AKI) to chronic kidney disease (CKD); the assessment of miRNA-21 in whole tissue homogenates, which fails to differentiate between cell types (such as tubular epithelial cells or infiltrating leukocytes); and the lack of functional manipulation of miRNA-21 to establish causality, also the inclusion of only male rats, our

[DOI: 10.47176/mjiri.40.68]

findings may not fully capture potential variations in female animals also. Future studies incorporating both sexes are warranted to address this limitation. These limitations hinder causal inferences and the potential for translational application, but they do not detract from the internal consistency of the observed protective effects.

Conclusion

This study demonstrated that pirfenidone and silymarin attenuate folic acid-induced acute kidney injury (AKI), with silymarin showing greater efficacy at the tested doses. The coordinated reduction in miRNA-21, markers of oxidative stress, and proinflammatory/pro fibrotic cytokines suggests that modulation of miRNA-21 is a plausible component of their renoprotective mechanisms. Future research should involve dose-response and pharmacokinetic studies, the protective combined effect of pirfenidone with silymarin in AKI, and longer follow-up to assess effects on AKI-to-CKD progression.

Acknowledgment

Not applicable.

Conflict of Interests

The authors declare that they have no competing interests.

Authors' Contributions

For this study, MHA was the primary supervisor and offered general scientific direction. The study's conceptualization and the experimental methodology's design were both influenced by NSA and AMT. AA and MEE created the experimental approach, carried out the laboratory procedures, and contributed to the idea of the study. Data processing, statistical analysis, and article drafting were the responsibilities of NSA, AMT, and MEE. MHA oversaw the study project's general supervision and performed histopathological evaluations. The paper was critically revised by all authors, who also evaluated and approved the final version for submission.

Ethical Considerations

Participation consent is not relevant. In compliance with ARRIVE recommendations and the Guide for the Care and Use of Laboratory Animals procedure (NIH publication), the investigational protocol was updated and authorized by the Institutional Animal Care and Use Committee, Helwan University (Approval number: 34-2023).

Funding Support

This study did not receive any specific financing from funding agencies in the public, commercial, or non-profit sectors.

Data Availability

The datasets used are available from the corresponding author on reasonable request.

AI Use Statement

AI tools were employed merely for grammar correction and language polishing. AI was not used in data collection, statistical analysis, or scientific interpretation. All intellectual contributions, conclusions, and accountability remain entirely with the authors.

References

1. Huang J, Chen J, Yang J, Han M, Xue Z, Wang Y, et al. Prediction models for acute kidney injury following liver transplantation: a systematic review and critical appraisal. Intensive Crit Care Nurs. 2025 Feb 1; 86:103808-103820.
2. Ashine TM, Mekonnen MS, Heliso AZ, Wolde YD, Babore GO, Bushen ZD, et al. Incidence and predictors of acute kidney injury among adults admitted to the medical intensive care unit of a comprehensive specialized hospital in central Ethiopia. PLoS One. 2024 Jun 26;19(6): e0304006.
3. Lv D, Jiang H, Yang X, Li Y, Niu W, Zhang D. Advances in understanding of dendritic cell in the pathogenesis of acute kidney injury. Front Immunol. 2024 Feb 16; 15:1294807.
4. Vallés PG, Gil Lorenzo AF, Garcia RD, Cacciamani V, Benardon ME, Costantino VV. Toll-like receptor 4 in acute kidney injury. Int J Mol Sci. 2023 Jan 11;24(2):1415-1435.
5. Cook N, Shepherd A, Boore J, Dunleavy S. Renal function and fluid balance. In: Disorder of homeostasis. Essentials of pathophysiology for nursing practice. 2nd ed. London: SAGE Publications; 2022. p.303-335.
6. Perazella MA, Rosner MH. Drug-induced acute kidney injury. Clin J Am Soc Nephrol. 2022 Aug 1;17(8):1220-1233.
7. Aguilar MG, AlHussen HA, Gandhi PD, Kaur P, Pothacamuri MA, Talikoti MA, et al. Sepsis-associated acute kidney injury: pathophysiology and treatment modalities. Cureus. 2024 Dec 19;16(12): e75992.
8. Zheng L, Chen X, Lin L, Guo H, Yang F. Bis-tetraarylimidazole macrocycle: an effective fluorescent sensor for folic acid. Dyes Pigments. 2025 May 1; 236:112691.
9. Powell BH, Witwer KW, Meffert MK. Cellular miRNAs and viruses: trends in miRNA sequestering and target de-repression. J Virol. 2025 Jun 18: e0091425.
10. Liechty C, Hu J, Zhang L, Liechty KW, Xu J. Role of microRNA-21 and its underlying mechanisms in inflammatory responses in diabetic wounds. Int J Mol Sci. 2020 May 8;21(9):3328.
11. Kim J, Ha S, Son M, Kim D, Kim MJ, Kim B, et al. TLR7 activation by miR-21 promotes renal fibrosis by activating the pro-inflammatory signaling pathway in tubule epithelial cells. Cell Commun Signal. 2023 Aug 18;21(1):215.
12. Li H, Xu M, Chen D, Wen W, Luo J. Pirfenidone ameliorates alcohol-induced promotion of breast cancer in mice. Front Oncol. 2024 Mar 25; 14:1351839.
13. Torre A, Martínez-Sánchez FD, Narvaez-Chávez SM, Herrera-Islas MA, Aguilar-Salinas CA, Córdova-Gallardo J. Pirfenidone use in fibrotic diseases: what do we know so far? Immun Inflamm Dis. 2024 Jul;12(7): e1335.
14. Zhao R, Xie B, Wang X, Zhang X, Ren Y, Wang C, et al. The tolerability and efficacy of antifibrotic therapy in patients with idiopathic pulmonary fibrosis: results from a real-world study. Pulm Pharmacol Ther. 2024 Mar 1; 84:102287.
15. Li W, Huang P, Wei J, Tan S, Liu G, Yang Q, Wang G. Down-regulation of miR-21-5p by pirfenidone to inhibit fibroblast proliferation in the treatment of acquired tracheal stenosis. Clin Respir J. 2024 Jan;18(1): e13727.
16. Jin Y, Wang X, Chen K, Chen Y, Zhou L, Zeng Y, et al. Silymarin decreases liver stiffness associated with gut microbiota in patients with metabolic dysfunction-associated steatotic liver disease: a randomized, double-blind, placebo-controlled trial. Lipids Health Dis. 2024 Aug 3;23(1):239.
17. Toghroli F, Noorbakhsh MF, Sajedianfard J. The effects of silymarin on calcium chloride-induced arrhythmia in male rats. Oxid Med Cell Longev. 2024; 2024:6720138.
18. Perez-Araluce M, Jüngst T, Sanmartin C, Prosper F, Plano D, Mazo MM. Biomaterials-based antioxidant strategies for the treatment of oxidative stress diseases. Biomimetics. 2024 Jan 3;9(1):23.
19. Faul F, Erdfelder E, Lang AG, Buchner A. G*Power 3: a flexible statistical power analysis program for the social, behavioral, and biomedical sciences. Behav Res Methods. 2007 May;39(2):175-191.
20. Zadeh MM, Ranji N, Motamed N. Deregulation of miR-21 and miR-155 and their putative targets after silibinin treatment in T47D breast cancer cells. Iran J Basic Med Sci. 2015 Dec;18(12):1209-1214.

[DOI: 10.47176/mjiri.40.68]

21. Manawy SM, Faruk EM, Hindawy RF, Hassan MM, Farrag DM, Bashar MA, et al. Modulation of the Sirtuin-1 signaling pathway in doxorubicin-induced nephrotoxicity (synergistic amelioration by resveratrol and pirfenidone). Tissue Cell. 2024 Apr 1; 87:102330.
22. Satyam SM, Bairy LK, Rehman A, Nair AA, Farook M, Binu NN, et al. Dapagliflozin and silymarin ameliorate cisplatin-induced nephrotoxicity via Nrf2/HO-1 upregulation: a preclinical mechanistic study. Sci. 2025 May 8;7(2):59-75.
23. Zaghlool SS, Abdelaal N, El-Shoura EA, Mahmoud NI, Ahmed YM. Restoring glomerular filtration rate by sulforaphane modulates ERK1/2/JNK/p38MAPK, IRF3/iNOS, and Nrf2/HO-1 signaling pathways against folic acid-induced acute renal injury in rats. Int Immunopharmacol. 2023 Oct 1; 123:110777.
24. Yan H, Xu J, Xu Z, Yang B, Luo P, He Q. Defining therapeutic targets for renal fibrosis: exploiting the biology of pathogenesis. Biomed Pharmacother. 2021 Nov 1; 143:112115.
25. Kölükçü E, Firat F, Deresoy FA, Katar M, Atılgan D. The effects of pirfenidone on ischemia-reperfusion injury in a testicular torsion-induced rat model. Andrologia. 2021 Mar;53(2):e13922.
26. Bozkurt I, Ozturk Y, Guney G, Arslan B, Gulbahar O, Guvenc Y, et al. Effects of pirfenidone on experimental head injury in rats. Int J Clin Exp Pathol. 2022 Jan 15;15(1):20-28.
27. Chandolia P, Rahi V, Kumar P. Neuroprotective effect of silymarin against 3-nitropropionic acid-induced neurotoxicity in rats. Curr Res Pharmacol Drug Discov. 2022 Jan 1; 3:100130.
28. Yu S, Chen X, Li X, Yan J, Jiang Y. Neuroprotective effects of CysLTR antagonist on Streptococcus pneumoniae-induced meningitis in rats. Exp Ther Med. 2022 May 13;24(1):443.
29. Lima-Posada I, Fontana F, Pérez-Villalva R, Berman-Parks N, Bobadilla NA. Pirfenidone prevents acute kidney injury in the rat. BMC Nephrol. 2019; 20:158.
30. Al-Shawi NN, Hussain SA, Hasson AH, Rashid YZ, Numan NA. The effect of different doses of silymarin on gentamicin-induced kidney damage in rats. Iraqi J Pharm Sci. 2024;33(1):45–53.
31. Zhou D, Sun Y, Dong C, Wang Z, Zhao J, Li Z, Huang G, Li W. Folic acid alleviated oxidative stress induced telomere attrition and inhibited apoptosis of neurocytes in old rats. Eur J Nutr. 2023; 63:291–302.
32. Gupta A, Shrman K, Kushwaha G, Goyal G, Singh G, Mansoori MS. Hepatoprotective activity of silymarin against paracetamol induced liver toxicity in albino rats. Pharma Innov J. 2023;12(7):1701–1705.
33. Paik SS, Lee JM, Ko IG, Kim SR, Kang SW, An J, Kim JA, Kim D, Hwang L, Jin JJ, Kim SH, Cha JY, Choi CW. Pirfenidone Alleviates Inflammation and Fibrosis of Acute Respiratory Distress Syndrome by Modulating the Transforming Growth Factor-β/Smad Signaling Pathway. Int J Mol Sci. 2024;25(15):8014-8026.
34. Nishikimi M, Rao NA, Yagi K. The occurrence of superoxide anion in the reaction of reduced phenazine methosulfate and molecular oxygen. Biochem Biophys Res Commun. 1972 Jan 31;46(2):849-854.
35. Ohkawa H, Ohishi N, Yagi K. Assay for lipid peroxides in animal tissues by thiobarbituric acid reaction. Anal Biochem. 1979 Jun 1;95(2):351-358.
36. Kiernan JA. Histological and histochemical methods: theory and practice. 5th ed. London: Arnold; 2015. p.132-212.
37. Emsley R, Dunn G, White IR. Mediation and moderation of treatment effects in randomized controlled trials of complex interventions. Stat Methods Med Res. 2010 Jun;19(3):237-270.
38. Bae CR, Kim Y, Kwon YG. CU06-1004 alleviates oxidative stress and inflammation on folic acid-induced acute kidney injury in mice. J Pharmacol Sci. 2024 Feb 1;154(2):77-85.
39. Karimian A, Mahmoudi L. Silymarin's potential in countering drug-induced cardiotoxicity, nephrotoxicity, and hepatotoxicity: a narrative review. Trends Pharm Sci Technol. 2024 Mar 1;10(1):15-24.
40. Abdulaal WH, Omar UM, Zeyadi M, El-Agamy DS, Alhakamy NA, Ibrahim SR, et al. Pirfenidone ameliorates ANIT-induced cholestatic liver injury via modulation of FXR, NF-κB/TNF-α, and Wnt/GSK-3β/β-catenin signaling pathways. Toxicol Appl Pharmacol. 2024 Sep 1; 490:117038.
41. Dahalia M, Gupta S, Majid H, Vohora D, Nidhi. Pirfenidone regulates seizures through the HMGB1/TLR4 axis to improve cognitive functions and modulate oxidative stress and neurotransmitters in PTZ-induced kindling in mice. Front Pharmacol. 2025 Jan 22; 15:1528032.
42. Shayestehyekta M, Moradi M. Graphene oxide and silymarin combination: a novel approach to improving post-cryopreservation quality of ram sperm. Cryobiology. 2025 Mar 1; 118:105199.
43. Bai L, Wang J, Wang X, Wang J, Zeng W, Pang J, et al. Combined therapy with pirfenidone and nintedanib counteracts fibrotic silicosis in mice. Br J Pharmacol. 2025 Mar;182(5):1143-1163.
44. Bava EP, George J, Tarique M, Iyer S, Sahay P, Aguilar BG, et al. Pirfenidone increases IL-10 and improves acute pancreatitis in multiple clinically relevant murine models. JCI Insight. 2022 Jan 25;7(2): e141108.
45. Guo HL, Liang XS, Zeng XP, Liu Y, Li ZS, Wang LJ, et al. Pirfenidone alleviates chronic pancreatitis via suppressing the activation of pancreatic stellate cells and the M1 polarization of macrophages. Int Immunopharmacol. 2024 Mar 30; 130:111691.
46. Zhao Y, Zhou Y, Gong T, Liu Z, Yang W, Xiong Y, et al. The clinical anti-inflammatory effects and underlying mechanisms of silymarin. iScience. 2024 Nov 15;27(11):111109.
47. Wang Y, Yang W, Yang Y, Liu X, Peng L, Huang Q, et al. Evidence construction of silibinin capsules against alcoholic liver disease based on a meta-analysis and systematic review. Front Pharmacol. 2025 Feb 4; 16:1516204.
48. Bakinowska E, Kiełbowski K, Pawlik A. The Role of MicroRNA in the Pathogenesis of Acute Kidney Injury. Cells. 2024 Sep 16;13(18):1559-1574.
49. Li W, Huang P, Wei J, Tan S, Liu G, Yang Q, Wang G. Down-regulation of miR-21-5p by pirfenidone to inhibit fibroblast proliferation in the treatment of acquired tracheal stenosis. Clin Respir J. 2024 Jan;18(1): e13727.
50. Henriet E, Abdallah F, Laurent Y, Guimpied C, Clement E, Simon M, et al. Targeting TGF-β1/miR-21 pathway in keratinocytes reveals protective effects of silymarin on imiquimod-induced psoriasis mouse model. JID Innov. 2022 Dec 16;3(3):100175.
51. Bylan D, Khalil A, Shebaby W, Habchy C, Nasser S, Faour WH, et al. Lebanese cannabis oil extract protected against folic acid-induced kidney fibrosis in rats. PLoS One. 2024 Dec 12;19(12): e0311790.
52. Sharawy MH, Serrya MS. Pirfenidone attenuates gentamicin-induced acute kidney injury by inhibiting inflammasome-dependent NLRP3 pathway in rats. Life Sci. 2020 Nov 1; 260:118454.
53. Attia HG, Mohamed BM, Alasmari SM, AbdelRahman SS, Aleraky M, Alqahtani A, et al. Effect of effervescent formulation of silymarin against experimental hepatotoxicity in rats: involvement of NRF2/HO-1, PI3K/AKT and TLR4/NFκB pathways. J Appl Vet Sci. 2025 Apr 1;10(2):18-27.
54. Deng Y, Zeng L, Liu H, Zuo A, Zhou J, Yang Y, et al. Silibinin attenuates ferroptosis in acute kidney injury by targeting FTH1. Redox Biol. 2024; 77:103360.

[DOI: 10.47176/mjiri.40.68]